

# The inclusion of MgH<sub>2</sub> into iron oxide and nickel oxide modified mesoporous carbon sorbent: an investigation on hydrogen production

Razie Dashti<sup>1</sup>, Javad Khodaveisi<sup>1</sup>, Seyyed Ershad Moradi<sup>2</sup>

<sup>1</sup>Young Researchers Club, Islamic Azad University – Bushehr Branch, Iran

<sup>2</sup>Young Researchers Club, Islamic Azad University – Sari Branch, Iran

## Abstract

In the present work, we investigated the hydrogen desorption properties of nano-sized MgH<sub>2</sub> that was loaded on ordered mesoporous carbon (OMC) surface that had been already modified with nickel and iron oxide nanoparticles. The surface modified mesoporous carbon was characterized by BET surface area and X-ray diffraction (XRD) analysis. The amount of MgH<sub>2</sub> on the carbon surface was confirmed by thermogravimetric analysis (TGA). Dehydrogenation data of MgH<sub>2</sub> on the ordered mesoporous carbon were collected for the pressure up to 8 MPa (80 bar) at 500 K. The incorporated MgH<sub>2</sub> on nickel oxide–mesoporous carbon nanocomposite had faster dehydrogenation kinetics compared to incorporated MgH<sub>2</sub> on iron oxide–mesoporous carbon nanocomposite as well as incorporated MgH<sub>2</sub> on mesoporous carbon. This can be attributed to the particle size of the former being smaller than that of the latter, as well as much accessible nanosized surface of loaded MgH<sub>2</sub>.

**Keywords:** mesoporous carbon, hydrogen desorption, MgH<sub>2</sub>, nanocomposite, iron oxide nanoparticle, nickel oxide nanoparticle.

Available online at the Journal website: <http://www.ache.org.rs/HI/>

SCIENTIFIC PAPER

UDC 661.846:66.017/.018

*Hem. Ind.* **66** (3) 317–325 (2012)

doi: 10.2298/HEMIND110929107B

Hydrogen is recognized as an environment-friendly fuel. Many researchers have recently focused their interests on the hydrogen generation by the new novel materials [1,2]. Alloys containing light elements are focused on high performance storage materials. Most hydrogen absorbing metals are very reactive, easily forming surface oxides, which then block the uptake of hydrogen. They also require costly and time-consuming activation. Magnesium, in particular, has a high storage capacity (7.6 wt.%) with the benefits of low cost and abundant availability [3]. The main barriers for the direct usage of pure MgH<sub>2</sub> are slow desorption kinetics, high thermodynamic stability and high reactivity toward air and oxygen, which it has in common with majority of lightweight metal hydrides [4–6].

Magnesium hydride is the binary metal hydride that comes closest to fuelling, in regard to the hydrogen storage density and stability as proposed by the U. S. Department of Energy [7]. However, magnesium hydride requires a temperature of approx. 280 °C for dehydrogenation at 1 bar ( $\Delta H_f = -75$  kJ/mol H<sub>2</sub>) and suffers from slow kinetics [7].

In recent years, significant progress has been made using nanocrystalline Mg produced by high energy milling [8] and with the addition of suitable catalysts [9–

–11]. For technical application, sufficiently fast kinetics have been achieved at 300 °C [10].

Recently, the preparation of nano-hydrides by ball milling techniques in a controlled environment and with further addition of submicro-nanoparticles dispersion of different additives such as transition metals, intermetallics or oxides, allowed the achievement of faster sorption kinetics at reduced temperatures [12–16]. At the same time the hydrogen sorption properties were investigated on model systems as Mg–Pd multilayer prepared by vacuum evaporation [17] or Nb-doped Mg films deposited by rf magnetron sputtering [18,19]. The phenomenological models explaining the observed improved kinetics of hydrogen sorption have advanced, taking into the account several factor such as the hydride grain-particle size [20], relevant surface area of oxide layers present in these nanosystems [21], the metal oxide particles dimension [21], the catalytic effect of some additives [22,23], and the thermal stability of the nanostructured hydrides against repeated absorption–desorption cycles [24]. Although the hydrogen diffusion mechanism at the nano-scale is not completely explained, recent investigations have indicated that suitable processing of MgH<sub>2</sub>-based nanocomposites is the way to modify hydrogen desorption channels with improved desorption properties, requiring cheaper but not strictly clean processing [25,26].

This required tremendous efforts made in the past decade that lead to the development of novel approaches, such as nanostructuring, alloying, and the use of catalysts [27–30]. It has been proven that high-

Correspondence: S.E. Moradi, Young Researchers Club, Islamic Azad University - Sari Branch 48164-194, Iran.

E-mail: er\_moradi@hotmail.com

Paper received: 29 September, 2011

Paper accepted: 12 December, 2011

energy ball milling could increase hydrogenation kinetics by reducing the particle size, activating the surface and introducing defects.

Additionally, Mg can be alloyed with other metallic elements, such as Ni to enhance the absorption kinetics, albeit at the cost of partial gravimetric capacity reduction [31]. Transitional metals such as Fe, Ti and V can lead to the catalyzation of hydrogen dissociation process and thus enhance the hydrogenation kinetics at high temperatures significantly (> 573 K) [26]. Recently, carbon materials, in particular carbon nanotubes, demonstrated having an excellent catalytic effect on hydrogen storage in Mg-based alloys by enhancing the hydrogen diffusion in MgH<sub>2</sub>-C or MgH<sub>2</sub>-metal-C systems [32–34].

Furthermore, great interest has been paid to the synthesis of nanosized metal hydrides in porous materials [35,36]. It has been suggested that incorporation of hydrogen storage materials into the micro- and mesoporous structure of nanoporous carbon materials would stabilize “nanosized” materials and prevent aggregation during cycling. Thus, the material would retain the thermodynamic parameters and kinetic behaviour associated with the hydrogenation-rehydrogenation of the nanomaterial rather than revert to the standard bulk material.

In this study, mesoporous carbons, iron oxide and nickel oxide modified mesoporous carbon have been impregnated with MgH<sub>2</sub>, using the organo-magnesium reagent, dibutylmagnesium (MgBu<sub>2</sub>) as the precursor. After being impregnated into mesoporous carbon pores, MgBu<sub>2</sub> was hydrogenated. The characterization and hydrogen storage properties of the resulting material were also examined. The MgH<sub>2</sub> nickel modified ordered mesoporous carbon (MgH<sub>2</sub>-OMC), MgH<sub>2</sub>-nickel modified ordered mesoporous carbon (MgH<sub>2</sub>-Ni-OMC) and MgH<sub>2</sub>-iron modified ordered mesoporous carbon (MgH<sub>2</sub>-Fe-OMC) systems were examined with respect to hydrogen sorption-desorption kinetics.

Here, we demonstrate new MgH<sub>2</sub>-Ni-OMC and MgH<sub>2</sub>-Fe-OMC systems that exhibit ultrafast hydrogenation kinetics with high capacity. A possible hydrogenation mechanism is proposed in terms of the synergistic catalytic effects of transition metals and OMC.

## EXPERIMENTAL

### Materials

The reactants used in this study were tetraethoxysilane (TEOS, 98%, Acros) as the silica source, non-ionic oligomeric alkyl-ethylene oxide surfactant (Pluronic 123) as the surfactant, HCl (35 wt.%), ethanol and deionized water for synthesis of mesoporous silica (SBA-15), sucrose as the carbon source, sulfuric acid as the catalyst for synthesis of mesoporous carbon, nickel

nitrate (NiNO<sub>3</sub>), ferrous iron and dibutylmagnesium MgBu<sub>2</sub> (1.0 M solution in heptanes) as the functionalization agents. All chemicals were of analytical grade from Merck.

### Adsorbent preparation

#### *Mesoporous silica and unmodified mesoporous carbon samples*

SBA-15 silica was prepared according to the procedure reported by Zhao *et al.* [37] with the use of a non-ionic oligomeric alkyl-ethylene oxide surfactant (Pluronic 123) as the structure-directing agent, after that the template was removed by means of calcinations at 500 °C in flowing air. Ordered porous carbon was synthesized *via* the two-step impregnation of the mesopores of SBA-15 with the solution of sucrose using the incipient wetness method [38]. Briefly, 1.0 g of the as-prepared SBA-15 was impregnated with the aqueous solution obtained by dissolving 1.1 g of sucrose and 0.14 g of H<sub>2</sub>SO<sub>4</sub> in 5.0 g of deionized water. The mixture was then dried at 100 °C for 6 h, and subsequently at 160 °C for 6 h. The silica sample, containing partially polymerized and carbonized sucrose, was treated again at 100 and 160 °C after the addition of 0.65 g of sucrose, 90 mg of H<sub>2</sub>SO<sub>4</sub> and 5.0 g of deionized water. The sucrose-silica composite was then heated at 900 °C for 4 h under nitrogen to complete the carbonization. The silica template was dissolved with 5 wt.% hydrofluoric acid at room temperature. The obtained template-free carbon product was filtered, washed with deionized water and ethanol, and dried.

#### *Iron oxide doped samples*

The prepared mesoporous carbon sorbent was used primarily as the supporting medium to prepare Fe-OMC by previously reported iron impregnation procedure [39]. The process used ferrous iron as the starting material, which could diffuse deep into the internal pores of OMC, followed by oxidation, which generates ferric iron that could cross-link with various functional groups in the dispersive way on the prepared OMC.

#### *Nickel doped samples*

The nanoporous carbon samples were impregnated with nickel nitrate (NiNO<sub>3</sub>) acetone solutions by the vacuum decomposition process using the incipient wetness impregnation method [40]. In this study, a nickel nitrate solution (analytical grade) of low concentration (5 mM) was selected for the vacuum impregnation process. The nanoporous carbon impregnated with the acetone solution was then filtered and dried at 60 °C for 4 h. The resultant nanoporous carbon doped with Ni was then heated at 100 °C for 1 h under hydrogen atmosphere with the goal of reducing the nickel salt to nanoparticles.

### MgH<sub>2</sub> doped samples

The mesoporous carbon samples (modified and unmodified iron oxide) were impregnated with MgBu<sub>2</sub> heptane solutions with the incorporated MgBu<sub>2</sub> then hydrogenated to MgH<sub>2</sub> [16]. The mesoporous carbon sample with a mass of 1.0 g was dried at 220 °C under vacuum for 5–6 h. After cooling down, the mesoporous carbon sample was transferred to an argon-purged glovebox and 20 ml of MgBu<sub>2</sub> was added. Subsequently, the solution and the mesoporous carbon sorbent were transferred and sealed into an autoclave with argon atmosphere, which was sustained by closing the valve that controls the outlet and inlet gas. The autoclave was brought out of the glovebox and then connected to the hydrogen gas line. Flushing the autoclave for 6–10 times with H<sub>2</sub> changed the argon atmosphere to hydrogen with H<sub>2</sub> pressure subsequently being adjusted to 4 MPa (40 bar). The autoclave was heated to 170 °C and the solution was stirred. After the temperature was reached and stabilized at 170 °C, the H<sub>2</sub> pressure was adjusted to 5–5.5 MPa (50–55 bar). With the end of hydrogenation, which lasted for ca. 24 h, the autoclave was cooled down to room temperature, the H<sub>2</sub> was vented and the autoclave was transferred into the glovebox. The autoclave was opened and black mesoporous carbons sorbent with gray fine precipitate of MgH<sub>2</sub> were observed. MgH<sub>2</sub> precipitate was decanted, washed out by pentane and removed with pipets. The remaining carbon–MgH<sub>2</sub> was dried at 85 °C under vacuum for 6 h.

### Textural and structural studies

The structure of the surface modified samples was investigated by powder X-ray diffraction (XRD) on a Philips 1830 diffractometer using graphite monochromated CuK $\alpha$  radiation. Adsorption isotherms of the mesoporous carbon samples were obtained using the N<sub>2</sub> gas microporosimeter (micromeritics model ASAP 2010 sorptometer) at 77 K. Pore size distribution and specific surface area were calculated by the Dollimore–Heal [41] and BET [42] methods. Pore volume was estimated from the amount of adsorbed N<sub>2</sub> gas at 0.963 in relative pressure, which derives from 25 nm radius pores. Micropore volume was calculated by t-plot. The thermal analysis was carried out using a NETZSCH STA449C analyzer. The instrument settings were: heating rate, 10 °C/min and a nitrogen atmosphere with 100 ml/min flow rate. For each measurement, about 25 mg of the ground adsorbent sample were used. The differential weight loss was calculated from the weight loss curve, where peaks represent the weight loss.

### Hydrogen adsorption-desorption

To study the hydrogen absorption kinetics the samples were placed in the closed system with constant volume under pure hydrogen atmosphere (99.995%). They were kept in vacuum at 250 °C during 5 h before the first absorption. The hydrogen initial pressure was set to 4 MPa (40 bar). The amount of absorbed hydrogen was estimated from the decrease of pressure with time. The successive hydrogen absorption/desorption kinetic measurements were performed at 300 °C (desorption).

The system used for thermal absorption/desorption process, utilizes a temperature controlled furnace and a fused silica tube where in hydrogen charged sample is heated at a constant rate under constant argon or hydrogen carrier flow. For subsequent analysis, the release argon and hydrogen gas was fed into the Hewlett-Packard gas chromatograph that permits quantitative analysis.

## RESULT AND DISCUSSION

### Pore textural properties

The isotherm is the most important information about surface and porosity obtained from the physisorption experiment. It reveals the kind of porosity present in porous and nonporous samples. Brunauer has defined five different types [42]. Type I isotherms are characteristic for microporous adsorbents, such as zeolites and carbons. Type IV isotherms are typical for mesoporous goods. Pore textural properties of the pure ordered mesoporous carbon, iron oxide and nickel oxide modified mesoporous carbons, and also MgH<sub>2</sub> modified carbons, were calculated from the nitrogen adsorption and desorption isotherms shown in Figure 1. It can be seen that after the modification, the obtained carbons continue to have type IV isotherms, indicating that mesoporosity is still preserved. However, the modification leads to a decrease in the total uptake of the mesoporous carbon, which reflects in the decrease of the total pore volume resulting from metal oxide and magnesium hydride nanoparticles modifications. Interestingly, the modified nanoporous carbons essentially keep the bimodal pore size distribution (*d* spacing have not changed much), which is characteristic for the parent mesoporous carbon. The textural parameters listed in Table 1 clearly confirm the structural changes of OMC to Fe–OMC, Ni–OMC, MgH<sub>2</sub>–OMC, MgH<sub>2</sub>–Ni–OMC and MgH<sub>2</sub>–Fe–OMC. Especially, the variations of the surface area and pore volume are significant by iron oxide nanoparticles loading.

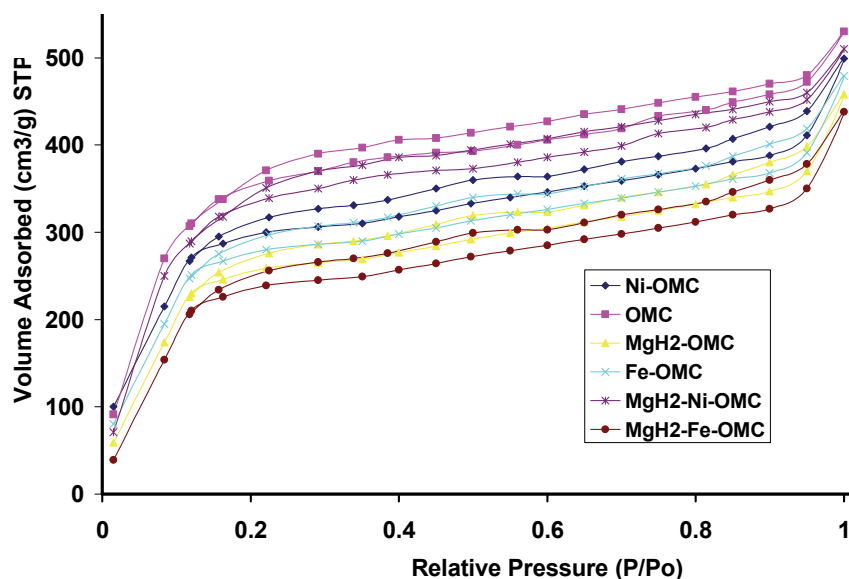


Figure 1. Adsorption-desorption isotherms of nitrogen at 77 K on OMC, Fe-OMC, Ni-OMC, MgH<sub>2</sub>-OMC, MgH<sub>2</sub>-Ni-OMC and MgH<sub>2</sub>-Fe-OMC.

Table 1. Textural parameters of the OMC, Fe-OMC, Ni-OMC, MgH<sub>2</sub>-OMC, MgH<sub>2</sub>-Ni-OMC and MgH<sub>2</sub>-Fe-OMC employed in this study;  $A_{BET}$  – specific surface area,  $V_p$  – pore volume

Adsorbent	$d$ Spacing, nm	$A_{BET} / m^2 g^{-1}$	$V_p / cm^3 g^{-1}$
OMC	3.7	1530	0.73
Ni-OMC	3.6	1467	0.72
Fe-OMC	3.6	1434	0.69
MgH <sub>2</sub> -OMC	3.5	1421	0.64
MgH <sub>2</sub> -Ni-OMC	3.5	1411	0.58
MgH <sub>2</sub> -Fe-OMC	3.4	1405	0.56

#### XRD Analysis

Figure 2 shows low angle XRD patterns of the parent mesoporous carbon and of MgH<sub>2</sub>-OMC, Ni-OMC and Fe-OMC samples. With OMC, three well-resolved peaks are observed, corresponding to the (100), (110) and (200) reflections typical of the 2D hexagonal space group  $P6mm$ . Along with all the replicas, the main reflection peak is well maintained, indicating that ordered mesoporous materials with hexagonal structures were obtained. For modified mesoporous samples, the

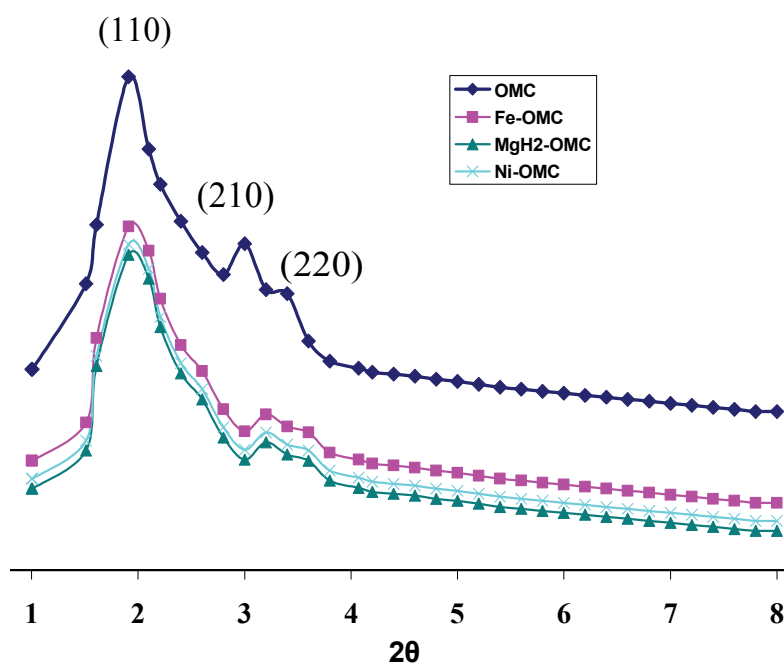


Figure 2. Low angle XRD patterns of the mesoporous carbon composite OMC, Ni-OMC, Fe-OMC and MgH<sub>2</sub>-OMC.

2D hexagonal structure of OMC was maintained well. However the XRD reflections become less than pristine, which can be the result of the partial damage of the mesoporous carbon sorbent.

The wide-angle XRD pattern of the studied MgH<sub>2</sub>-OMC is shown in Figure 3. The XRD spectra of the Fe-OMC and Ni-OMC have also been recorded for comparison. The wide-angle XRD patterns of nickel modified mesoporous adsorbent (Ni-OMC) in Figure 3 exhibit two resolved diffraction peaks at 44.59 (111) and 51.90° (200) 2θ, characteristic of metallic nickel with the fcc structure. It reveals that the nickel species in the mesoporous carbon matrix exists in metallic form. The weak and broad peak at 2θ = 35° of the Fe-OMC sample corresponds to almost very small iron (III) oxide crystallites.

The MgH<sub>2</sub> incorporated mesoporous carbon (MgH<sub>2</sub>-OMC) shows two broad diffraction peaks (2θ = 26.5° and 37°), implying that the incorporated MgH<sub>2</sub> has a very small particle size. Therefore, XRD results indicate that incorporated MgH<sub>2</sub> has been confined in the pore structure of mesoporous carbons.

#### TGA analysis

Figure 4 shows thermogravimetric analysis (TGA) curve of the mesoporous carbons using nitrogen atmo-

sphere and heating rate of 10 °C min<sup>-1</sup> ranging from the room temperature to 1000 °C. Subsequently, the carbon and magnesium hydride were oxidized to CO<sub>2</sub> and MgO, respectively. The weight loss at 280–650 °C is attributed to the decomposition of carbon in nitrogen. The weight of the samples at 650 °C is about 15, 3 and 19% of the starting MgH<sub>2</sub>-OMC, Fe-OMC and MgH<sub>2</sub>-Fe-OMC, respectively. Assuming that almost all the residual is from MgH<sub>2</sub>, it can be calculated that MgH<sub>2</sub> loading is 15 wt.% related to the total weight of the incorporated material.

#### Hydrogen desorption analysis

##### Temperature effect

The quantification of the hydrogen desorption for the MgH<sub>2</sub>-Ni-OMC and MgH<sub>2</sub>-Fe-OMC systems is given in Figure 5 together with that of MgH<sub>2</sub>-OMC. The data were obtained by measuring the amount of desorbed hydrogen every 20 °C, ranging from room temperature to 300 °C, using a volumetric apparatus. The calibrated volume, in which hydrogen was collected, was regularly emptied so to maintain the pressure below 0.1 MPa (1 bar). For each temperature, the measurement of the hydrogen desorption capacity was made after the total release duration of 15 h. The final hydrogen desorption capacity at 300 °C for MgH<sub>2</sub>-OMC, MgH<sub>2</sub>-Ni-OMC and

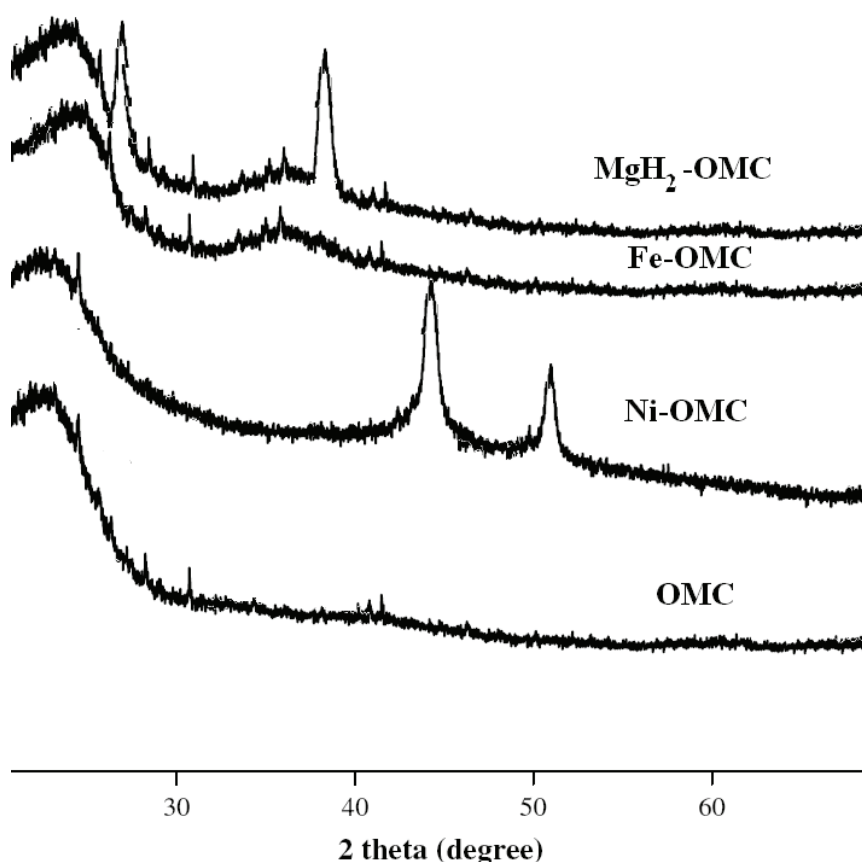


Figure 3. Wide angle XRD patterns of the mesoporous carbon composite OMC, Ni-OMC, Fe-OMC and MgH<sub>2</sub>-OMC.

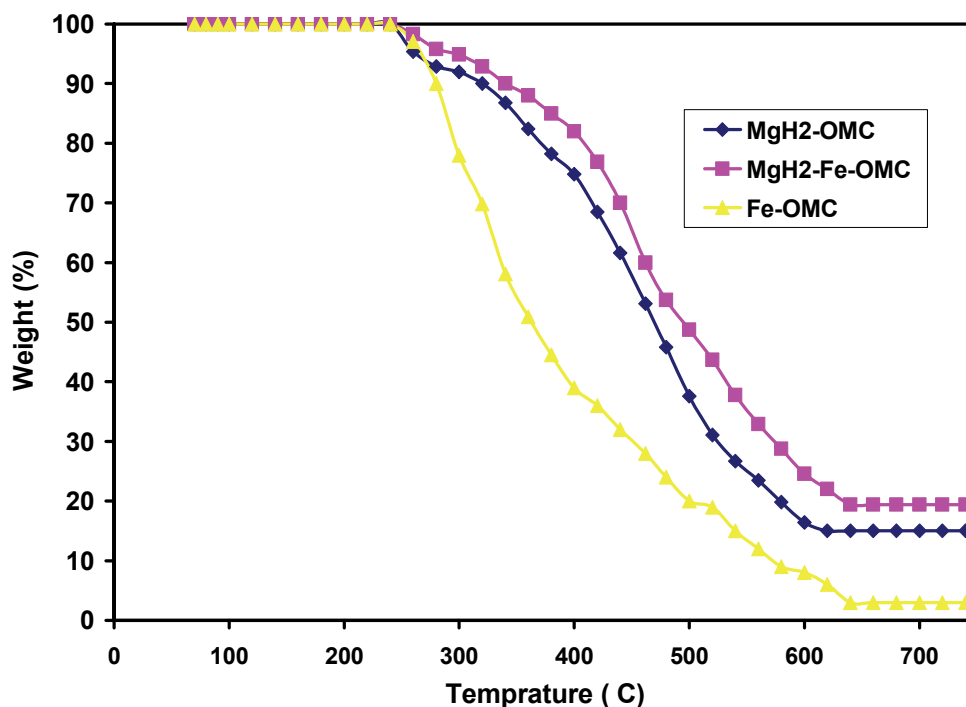


Figure 4. TGA curve of MgH<sub>2</sub> incorporated mesoporous carbon composite. The samples were heated under nitrogen atmosphere with a heating rate of 10 °C min<sup>-1</sup>.

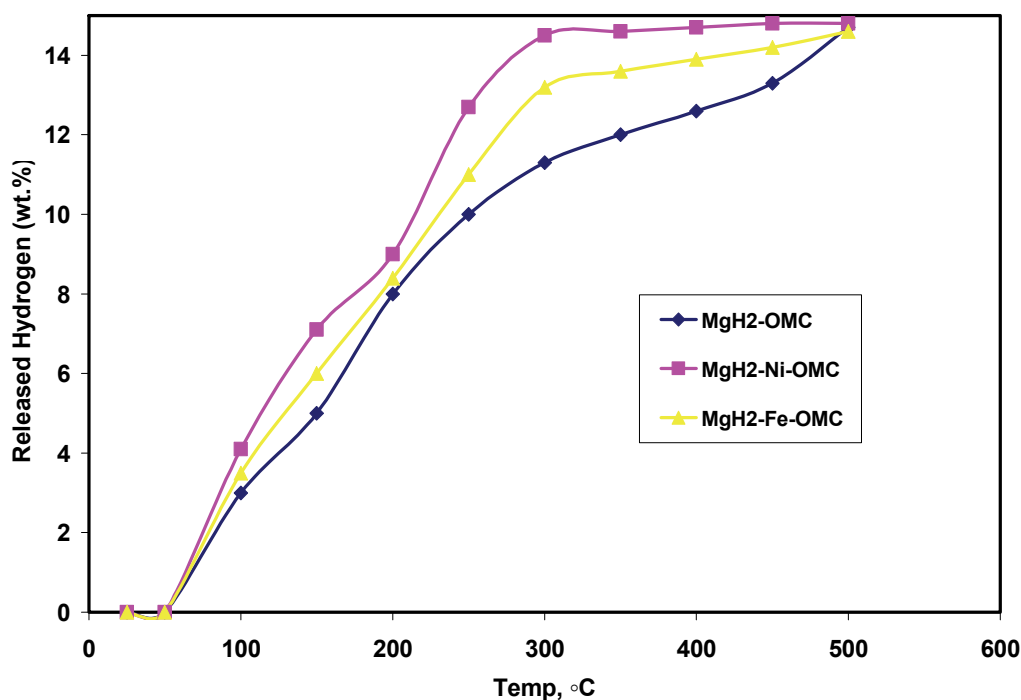


Figure 5. Amounts of released hydrogen at different temperatures for MgH<sub>2</sub>-OMC, MgH<sub>2</sub>-Ni-OMC and MgH<sub>2</sub>-Fe-OMC.

MgH<sub>2</sub>-Fe-OMC reaches 11.3, 14.5 and 13.2 wt.%, respectively. Complete achievement of the desorption process for MgH<sub>2</sub>-OMC, MgH<sub>2</sub>-Ni-OMC and MgH<sub>2</sub>-Fe-OMC requires higher temperatures and/or longer durations. The positive effect exhibited by the MgH<sub>2</sub> confinement to nanoscale is its capability to release hydro-

gen at temperatures as low as 200 °C. The total hydrogen desorption capacity at 500 °C is near to 12.0% per weight of MgH<sub>2</sub> (for MgH<sub>2</sub>-OMC). It can be concluded that the desorbed material is also embedded into the mesoporous carbon since no reflections are visible, apart for those as the effect of sample holder. The carbo-

naceous host is therefore able to maintain the confinement of the material during the desorption process.

#### Effect of surface oxide on kinetics

The isothermal dehydrogenation kinetic experiments of pore MgH<sub>2</sub>, MgH<sub>2</sub>-OMC, MgH<sub>2</sub>-Ni-OMC and MgH<sub>2</sub>-Fe-OMC at 280 °C has been done, in which the amount of desorbed hydrogen was normalized as the wt.% related to MgH<sub>2</sub> (Figure 6). Based on the hydrogen evolution in the first hour of dehydrogenation, the initial dehydrogenation rates are 9.1, 12.1 and 13.2 wt.% h<sup>-1</sup> for the MgH<sub>2</sub>-OMC, MgH<sub>2</sub>-Ni-OMC and MgH<sub>2</sub>-Fe-OMC, respectively. For all of MgH<sub>2</sub> incorporated in mesoporous carbon, dehydrogenation at 280 °C is almost complete in 8 h with about 2 wt.% hydrogen evolution. The fast dehydrogenation rate of incorporated MgH<sub>2</sub> can be attributed to the small hydride size that was confined by the porous structure of the mesoporous carbon. It should be noted that the dehydrogenation kinetics for the nanosized incorporated MgH<sub>2</sub> and pore MgH<sub>2</sub> are slower than those initially observed with MgH<sub>2</sub> containing Ni or Fe catalyst [43].

hydrogen storage applications. The MgH<sub>2</sub>-Ni-OMC is also found to be more effective than others for the hydrogen desorption from MgH<sub>2</sub>.

#### Acknowledgments

We gratefully acknowledge financial support received from Iran Renewable Energy Organization (SUNA).

#### REFERENCES

- [1] A. Zuttel, Hydrogen storage methods, *Naturwissenschaften* **91** (2004) 157–172.
- [2] L. Schlapbach, A. Zuttel, Hydrogen-storage materials for mobile applications, *Nature* **414** (2001) 353–358.
- [3] G. Liang, J. Huot, S. Boily, A. Van Neste, R. Schulz, Catalytic effect of transition metals on hydrogen sorption in nanocrystalline ball milled MgH<sub>2</sub>-Tm (Tm = Ti, V, Mn, Fe and Ni) systems, *J. Alloys Compd.* **292** (1999) 247–252.
- [4] L. Ma, P. Wang, H. Cheng, Improving hydrogen sorption kinetics of MgH<sub>2</sub> by mechanical milling with TiF<sub>3</sub>, *J. Alloys Compd.* **432** (2007) L1-L4.
- [5] X. Yao, C. Wu, G. Lu, H. Cheng, S. Smith, J. Zou, Y. He,

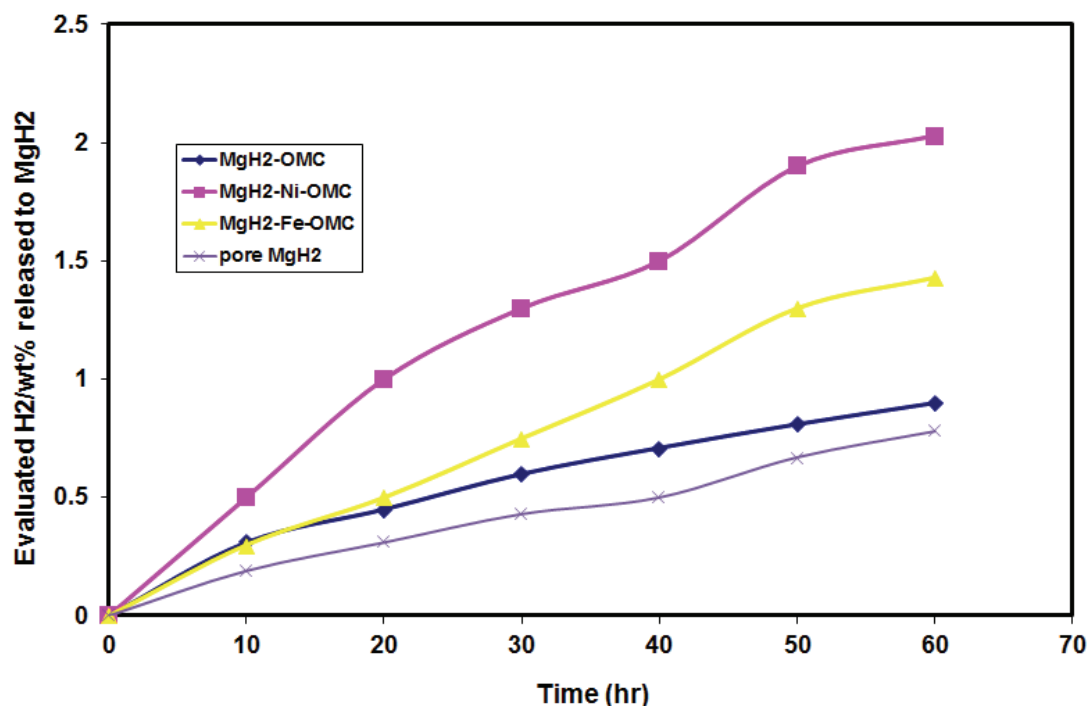


Figure 6. Isothermal dehydrogenation kinetics at 280 °C of pure MgH<sub>2</sub>, MgH<sub>2</sub>-OMC, MgH<sub>2</sub>-Ni-OMC and MgH<sub>2</sub>-Fe-OMC.

#### CONCLUSION

In conclusion, we demonstrated that transition metals significantly enhance the hydrogen kinetics while mesoporous structure remarkably increases the capacity. A new MgH<sub>2</sub>-Ni-OMC and MgH<sub>2</sub>-Fe-OMC system were shown to have very fast dehydrogenation kinetics and very large capacity, which is very promising for

Mg-Based nanocomposites with high capacity and fast kinetics for hydrogen storage, *J. Phys. Chem., B* **110** (2006) 11697–11703.

- [6] V. Berube, G. Radtke, M.S. Dresselhaus, G. Chen, Size effects on the hydrogen storage properties of nanostructured metal hydrides: A review, *Int. J. Energy Res.* **31** (2007) 637–663.

- [7] US Department of Energy. <http://www.eere.energy.gov/hydrogenandfuelcells/hydrogen/-storage.html>.
- [8] K. Shindo, T. Kondo, M. Arakawa, Y. Sakurai, Hydrogen adsorption/desorption properties of mechanically milled activated carbon, *J. Alloys Compd.* **359** (2003) 267–271.
- [9] K.F. Aguey-Zinsou, J.R. Ares Fernandez, T. Klassen, R. Bormann, Effect of Nb<sub>2</sub>O<sub>5</sub> on MgH<sub>2</sub> properties during mechanical milling, *Int. J. Hydrogen Energy* **32** (2007) 2400–2407.
- [10] A. Montone, J. Grbović, Lj. Stamenković, A.L. Fiorini, L. Pasquini, E. Bonetti, M.V. Antisari, Desorption behaviour in nanostructured MgH<sub>2</sub>-Co, *Mat. Sci Forum.* **518** (2006) 79–84.
- [11] A. Zaluska, L. Zaluski and J. Strom-Olsen, Nanocrystalline magnesium for hydrogen storage, *J. Alloys Compd.* **288** (1999) 217–225.
- [12] R.A. Varin, T. Czujko, C. Chiu and Z. Wronski, Particle size effects on the desorption properties of nanostructured magnesium dihydride (MgH<sub>2</sub>) synthesized by controlled reactive mechanical milling (CRMM), *J. Alloys Compd.* **424** (2006) 356–364.
- [13] P.-A. Huhn, M. Dornheim, T. Klassen and R. Bormann, Thermal stability of nanocrystalline magnesium for hydrogen storage, *J. Alloys Compd.* **404–406** (2005) 499–502.
- [14] F. Schuth, B. Bogdanovic, A. Taguchi 2003 Patent Application WO2005014469
- [15] J.L. Bobet, E. Akiba, B. Darriet, Study of Mg-M (M=Co, Ni and Fe) mixture elaborated by reactive mechanical alloying: hydrogen sorption properties, *Int. J. Hydrogen Energy* **26** (2001) 493–501.
- [16] A.F. Gross, J.J. Vajo, S.L. Van Atta, G.L. Olson, Enhanced hydrogen storage kinetics of LiBH<sub>4</sub> in nanoporous carbon scaffolds, *J. Phys. Chem., C* **112** (2008) 5651–5657.
- [17] H. Fujii, S.Orimo, Hydrogen storage properties in nanostructured magnesium- and carbon-related materials, *Physica, B* **328** (2003) 77–80.
- [18] N. Bazzanella, R. Checchetto, A. Miotello, G.Sada, P. Mazzoldi, P. Mengucci, Hydrogen kinetics in magnesium hydride: On different catalytic effects of niobium, *Appl. Phys. Lett.* **89** (2006) 014101–014103.
- [19] R. Checchetto, N. Bazzanella, A. Miotello, C. Maurizio, F. D’Acapito, P. Mengucci, G. Barucca, and G. Majni, Nb clusters formation in Nb-doped magnesium hydride, *Appl. Phys. Lett.* **87** (2005) 061904–061906.
- [20] R.A. Varin, T.Kzujko, Z.Wronski, Particle size, grain size and g-MgH<sub>2</sub> effects on the desorption properties of nanocrystalline commercial magnesium hydride (MgH<sub>2</sub>) processed by controlled mechanical milling, *Nanotechnology* **17** (2006) 3856–3865.
- [21] O. Friedrichs, J.C. Sánchez-López, C. López-Cartes, M. Dornheim, T. Klassen, R. Bormann, A. Fernandez, Chemical and microstructural study of the oxygen passivation behaviour of nanocrystalline Mg and MgH<sub>2</sub>, *Appl. Surf. Science* **252** (2006) 2334–2335.
- [22] N. Hanada, T. Ichikawa, H. Fujii, Catalytic effect of nanoparticle 3d-transition metals on hydrogen storage properties in magnesium hydride mgH<sub>2</sub> prepared by mechanical milling, *J. Phys. Chem., B* **109** (2005) 7188–7194.
- [23] J. Huot, G. Liang, R. Schultz, Mechanically alloyed metal hydride systems, *Appl. Phys., A* **72** (2001) 187–195.
- [24] H.G. Schimmel, J. Huot, L.C. Chapon, F.D. Tichelaar, F.M. Mulder, Hydrogen cycling of niobium and vanadium catalyzed nanostructured magnesium J. Am. Chem. Soc. **127** (2005) 14348–14354.
- [25] A. Ranjbar, M. Ismail, Z.P. Guo, X.B. Yu, H.K. Liu, Effects of CNTs on the hydrogen storage properties of MgH<sub>2</sub> and MgH<sub>2</sub>-BCC composite, *Int. J. Hydrogen Energy* **35** (2010) 7821–7826.
- [26] C.X. Shang, Z.X.J. Guo, Effect of carbon on hydrogen desorption and absorption of mechanically milled MgH<sub>2</sub>, *J. Power Sources* **129** (2004) 73–80.
- [27] A.M. Seayad, D.M. Antonelli, Recent advances in hydrogen storage in metal-containing inorganic nanostructures and related materials, *Adv. Mater.* **16** (2004) 765–777.
- [28] M. Hirscher, M.J. Becher, Hydrogen storage in carbon nanotubes, *Nanosci. Nanotechnol.* **3** (2003) 3–17.
- [29] W. Oelerich, T. Klassen, R.J. Bormann, Metal oxides as catalysts for improved hydrogen sorption in nanocrystalline Mg-based materials, *J. Alloys Compd.* **315** (2001) 237–242.
- [30] L. Zaluski, A. Zaluska, J.O. Strom-Olsen, Catalytic effect of Pd on hydrogen absorption in mechanically alloyed Mg<sub>2</sub>Ni, LaNi<sub>5</sub> and FeTi, *J. Alloys Compd.* **217** (1995) 295–300.
- [31] S. Yasuoka, Y. Magari, T. Murata, T. Tanaka, J. Ishida, H. Nakamura, T. Nohma, M. Kihara, Y. Bab, H. Teraoka, Development of high-capacity nickel-metal hydride batteries using superlattice hydrogen-absorbing alloys, *J. Power Sources* **156** (2006) 662–666.
- [32] S. Orimo, H. Fuji, Materials science of Mg-Ni-based new hydrides, *Appl. Phys. A* **72** (2001) 167–186.
- [33] G. Urretavizcaya V. Fuster, F.J. Castro, High pressure DSC study of hydrogen sorption in MgH<sub>2</sub>/graphite mixtures: Effects of sintering and oxidation, *Int. J. Hydrogen Energy* **36** (2011) 5411–5417.
- [34] C.Z. Wu, P. Wang, X. Yao, C. Liu, D.M. Chen, G.Q. Lu, H.M. Cheng, Effect of carbon/noncarbon addition on hydrogen storage behaviors of magnesium hydride, *J. Alloys Compd.* **414** (2006) 259–264.
- [35] P.E. de Jongh, R.W.P. Wagemans, T.M. Eggenhuisen, B.S. Dauvillier, P.B. Radstake, J.D. Meeldijk, J.W. Geus and K.P. de Jong, The Preparation of carbon-supported magnesium nanoparticles using melt infiltration, *Chem. Mater.* **19** (2007) 6052–6057.
- [36] A.F. Gross, C.C. Ahn, S.L. van Atta, P. Liu, J.J. Vajo, Fabrication and hydrogen sorption behaviour of nanoparticulate MgH<sub>2</sub> incorporated in a porous carbon host, *Nanotechnology* **20** (2009) 204005–204010.
- [37] D. Zhao, J. Feng, Q. Huo, N. Melosh, G.H. Fredrickson, B.F. Chmelka, G. Stucky, Triblock copolymer syntheses of mesoporous silica with periodic 50 to 300 angstrom pores, *Science* **279** (1998) 548–552.
- [38] S. Jun, S.H. Joo, R. Ryoo, M. Kruk, M. Jaroniec, Z. Liu, T. Ohsuna, O. Terasaki, Synthesis of new, nanoporous carbon with hexagonally ordered mesostructure *J. Am. Chem. Soc.* **122** (2000) 10712–10713.



- [39] Z. Gu, J. Fang, B. Deng, Preparation and evaluation of GAC-based iron-containing adsorbents for arsenic removal, *Environ. Sci. Technol.* **39** (2005) 3833–3843.
- [40] H. Li, S. Zhu, H. Xi, R. Wang, Nickel oxide nanocrystallites within the wall of ordered mesoporous carbon CMK-3: Synthesis and characterization, *Micropor. Mesopor. Mater.* **89** (2006) 196–203.
- [41] U. Ciesla, F. Schüth, Ordered mesoporous materials, *Micropor. Mesopor. Mater.* **27** (1999) 131–149.
- [42] A. Saito, H.C. Foley, Curvature and parametric sensitivity in models for adsorption in micropores, *AIChE J.* **37** (1991) 429–436.
- [43] C. Wu, P. Wang, X. Yao, C. Liu, D. Chen, G.Q. Lu and H. Cheng, Effects of SWNT and metallic catalyst on hydrogen absorption/desorption performance of MgH<sub>2</sub>, *J. Phys. Chem., B* **109** (2005) 22217–22221.

## IZVOD

### INKLUZIJA MgH<sub>2</sub> U MEZOPOROZNI GRAFITNI SORBENT MODIFIKOVAN GVOŽĐE-OKSIDOM I NIKAL-OKSIDOM: ISPITIVANJE PROIZVODNJE VODONIKA

Razie Dashti<sup>1</sup>, Javad Khodaveisi<sup>1</sup>, Seyyed Ershad Moradi<sup>2</sup>

<sup>1</sup>*Young Researchers Club, Islamic Azad University – Bushehr Branch, Iran*

<sup>2</sup>*Young Researchers Club, Islamic Azad University – Sari Branch, Iran*

(Naučni rad)

U ovom radu, ispitivano je desorpciono ponašanje nanostrukturnog MgH<sub>2</sub> koji je formiran na uređenoj površini mezoporoznog ugljenika (OMC), koja je prethodno modifikovana sa česticama oksida gvožđa i nikla. Karakterizacija modifikovane površine mezoporoznog ugljenika je rađena BET i rendgenskom strukturnom (XRD) analizom. Količina MgH<sub>2</sub> na površini ugljenika je potvrđena termogravimetrijskom analizom (TGA). Podaci o dehidrogenaciji MgH<sub>2</sub> sa uređenog mezoporoznog ugljenika su dobijeni za pritisak od 8 MPa i temperaturu od 500 K. Utvrđeno je da je kinetika dehidrogenacije brža sa površine modifikovane nikal-oksikom u odnosu na onu modifikovanu gvožđe-oksikom. Ovi eksperimentalni rezultati se mogu objasniti činjenicom da je veličina čestica nanokompozita nikal-oksik/mezoporozni ugljenik manja nego nanokompozita dobijenog sa gvožđe-oksikom, kao i većom dostupnošću nanostrukturne površine inkorporiranog MgH<sub>2</sub>.

*Ključne reči:* Mezoporozni ugljenik • Desorpcija vodonika • MgH<sub>2</sub> • Nanokompozit • Nanačestica gvožđe-oksida • Nanačestica nikal-oksida